Supporting Information

Comprehensive Understanding of Ethylene Epoxidation on Copper Catalysts: A Microkinetic Study with Coverage Effects

Zhuozheng Wang,[1,2,3] Wenbo Xie[2,3] Yarong Xu,[4] Yulan Han,[3] Jiayan Xu,[3] P. Hu*[2,3]

[1]PetroChina Petrochemical Research Institute, Beijing 102206, China

[2]School of Physical Science and Technology, ShanghaiTech University, 393 Middle Huaxia Road, Shanghai 201210, China

[3]School of Chemistry and Chemical Engineering, The Queen's University of Belfast, Belfast BT9 5AG, United Kingdom

[4]Research Institute of Urumqi Petrochemical Company, PetroChina Company Limited, Urumqi 830019, China

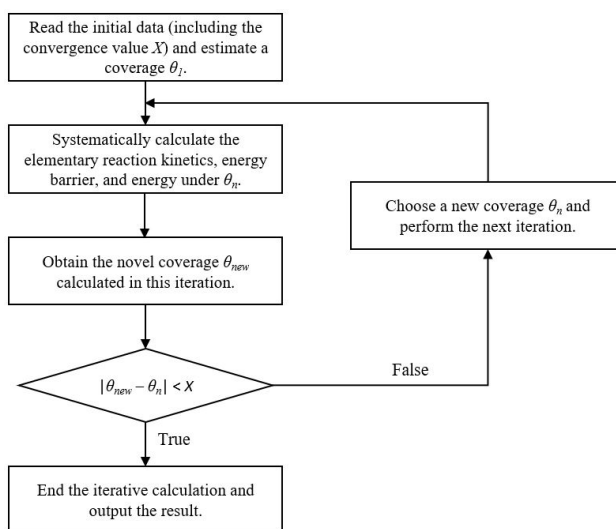## S1. Logical diagrams of the self-consistent microkinetic modeling

Figure S1 The logical flow diagram of self-consistent microkinetic model utilized in this work.

S2. Optimized structures of adsorbate-adsorbate cross-interactions and transition state cross-interactions
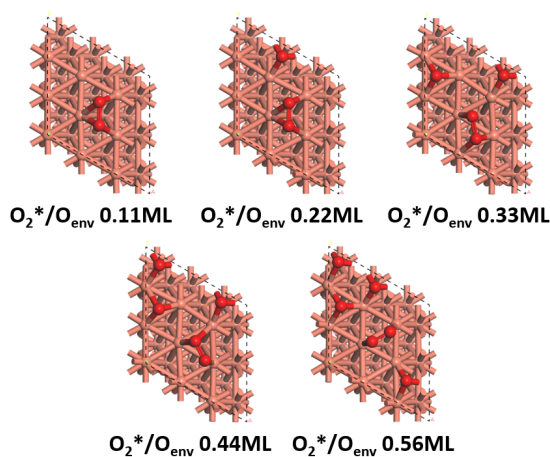

O_2*/O_{env} 0.11ML O_2*/O_{env} 0.22ML O_2*/O_{env} 0.33ML

O_2*/O_{env} 0.44ML O_2*/O_{env} 0.56ML

Figure S2 Structures of O_2*/O_{env} at the coverage from 0.11 ML to 0.56 ML. The color code: red, oxygen; brown, copper.

OME*/O$_{env}$ 0.11ML   OME*/O$_{env}$ 0.22ML   OME*/O$_{env}$ 0.33ML

OME*/O$_{env}$ 0.44ML   OME*/O$_{env}$ 0.56ML   OME*/O$_{env}$ 0.67ML
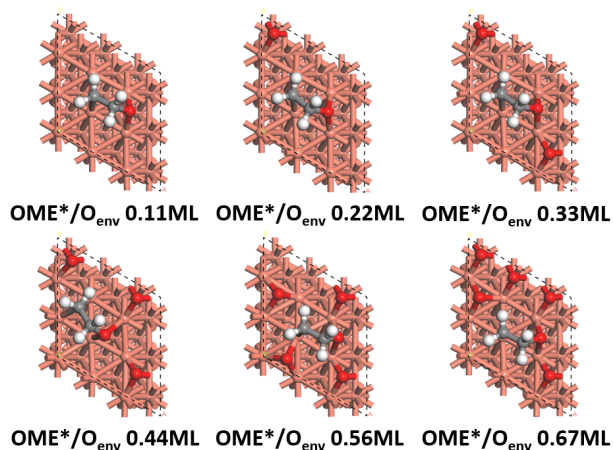
Figure S3 Structures of OME*/O$_{env}$ at the coverage from 0.11 ML to 0.67 ML. The color code: red, oxygen; white, hydrogen; dark grey, carbon; brown, copper.
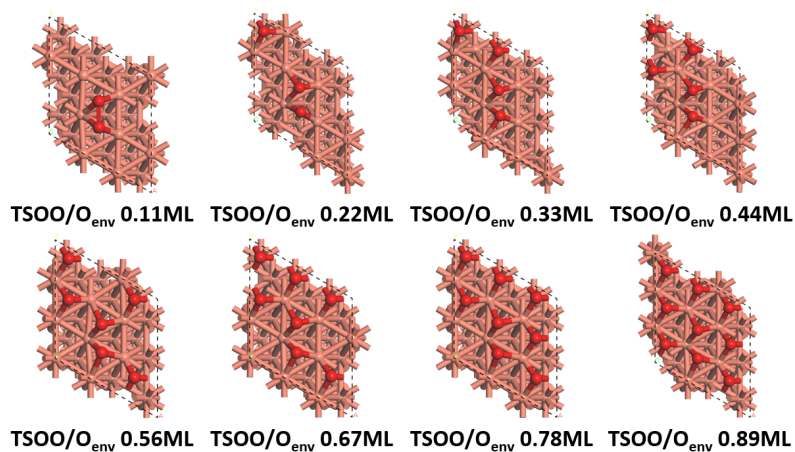
TSOO/O$_{env}$ 0.11ML   TSOO/O$_{env}$ 0.22ML   TSOO/O$_{env}$ 0.33ML   TSOO/O$_{env}$ 0.44ML

TSOO/O$_{env}$ 0.56ML   TSOO/O$_{env}$ 0.67ML   TSOO/O$_{env}$ 0.78ML   TSOO/O$_{env}$ 0.89ML

Figure S4 Structures of TSOO/O$_{env}$ at the coverage from 0.11 ML to 0.89 ML. The color-coding is the same as **Figure S3**.

TS1/O$_{env}$ 0.11ML   TS1/O$_{env}$ 0.22ML   TS1/O$_{env}$ 0.33ML   TS1/O$_{env}$ 0.44ML

TS1/O$_{env}$ 0.56ML   TS1/O$_{env}$ 0.67ML   TS1/O$_{env}$ 0.78ML   TS1/O$_{env}$ 0.89ML

Figure S5 Structures of TS1/O$_{env}$ at the coverage from 0.11 ML to 0.89 ML. The color-coding is the same as **Figure S3**.

TSEO/O$_{env}$ 0.11ML   TSEO/O$_{env}$ 0.22ML   TSEO/O$_{env}$ 0.33ML   TSEO/O$_{env}$ 0.44ML
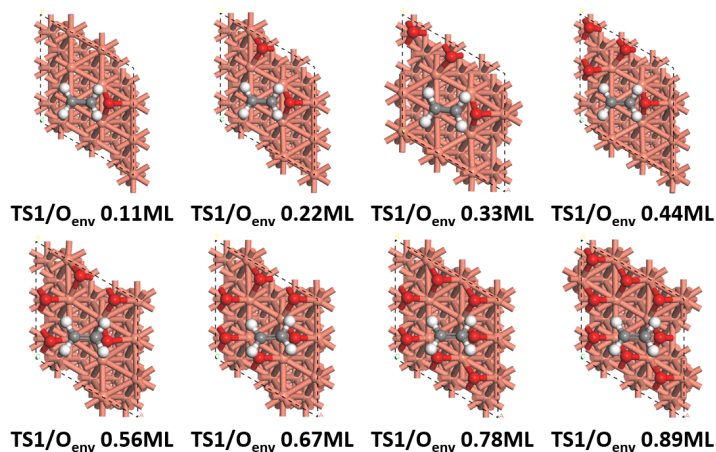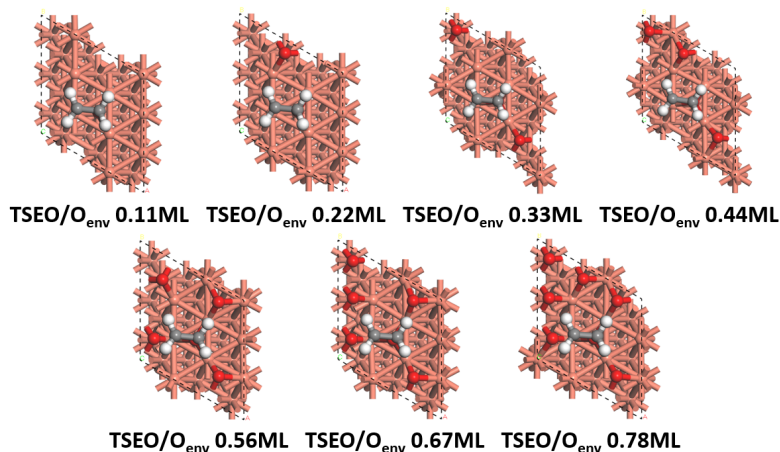
TSEO/O$_{env}$ 0.56ML   TSEO/O$_{env}$ 0.67ML   TSEO/O$_{env}$ 0.78ML

Figure S6 Structures of TSEO/O$_{env}$ at the coverage from 0.11 ML to 0.78 ML. The color-coding is the same as **Figure S3**.

TSAA/O$_{env}$ 0.11ML   TSAA/O$_{env}$ 0.22ML   TSAA/O$_{env}$ 0.33ML
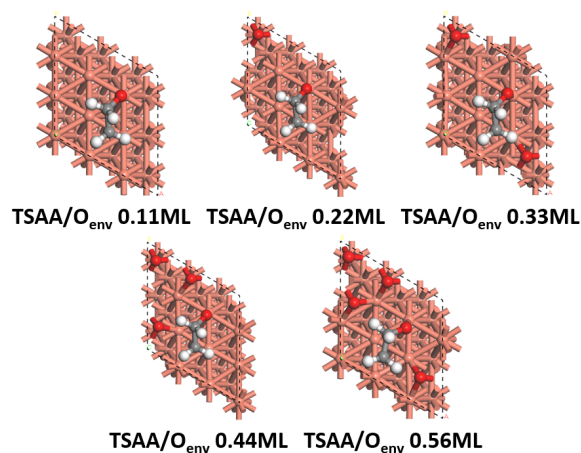
TSAA/O$_{env}$ 0.44ML   TSAA/O$_{env}$ 0.56ML

Figure S7 Structures of TSAA/O$_{env}$ at the coverage from 0.11 ML to 0.56 ML. The color-coding is the same as **Figure S3**.

S3. Coverage-dependent linear relationships of chemisorption energy with coverage

Table S1 The two-line model: List of all adsorbate interactions under high coverage from 480 K to 600 K on Cu(111).

	O*/O_{env}	O_2*/O_{env}	OME*/O_{env}
480 K	y = 4.957x - 0.097	y = 7.648x + 1.809	y = 7.792x + 0.386
490 K	y = 4.957x - 0.092	y = 7.692x + 1.803	y = 7.818x + 0.396
500 K	y = 4.945x - 0.076	y = 7.692x + 1.813	y = 7.818x + 0.396
520 K	y = 4.938x - 0.067	y = 7.692x + 1.823	y = 7.792x + 0.416
540 K	y = 4.926x - 0.056	y = 7.651x + 1.841	y = 7.792x + 0.441
600 K	y = 4.903x - 0.021	y = 7.607x + 1.897	y = 7.783x + 0.493

Table S2 The two-line model: List of all transition state interactions under high coverage from 480 K to 600 K on Cu(111).

	TSOO/O_{env}	TS1/O_{env}	TSEO/O_{env}	TSAA/O_{env}
480 K	y = 7.297x + 2.562	y = 4.470x + 2.459	y = 2.840x + 2.961	y = 5.520x + 2.133
490 K	y = 7.304x + 2.575	y = 4.480x + 2.473	y = 2.849x + 2.974	y = 5.519x + 2.157
500 K	y = 7.320x + 2.579	y = 4.475x + 2.476	y = 2.858x + 2.971	y = 5.520x + 2.153
520 K	y = 7.277x + 2.618	y = 4.457x + 2.489	y = 2.822x + 2.995	y = 5.520x + 2.163
540 K	y = 7.277x + 2.628	y = 4.465x + 2.512	y = 2.849x + 3.004	y = 5.476x + 2.209
600 K	y = 7.244x + 2.686	y = 4.430x + 2.567	y = 2.849x + 3.042	y = 5.432x + 2.275

S4. Formation energies

Parameterizing classical energies can reduce errors in simulations while ensuring thermodynamic consistency for complex surface catalytic reactions such as ethylene epoxidation. The generalized formation energies and corresponding energies of species have been completely developed and precisely applied,[1] which are applicable to the ethylene epoxidation system in this work:

$$
\begin{aligned}
R_H &= \frac{1}{2}\left(U_{H_2}\right) \\
R_C &= U_{CH_4} - 4R_H \\
R_O &= U_{H_2O} - 2R_H
\end{aligned}
\qquad \text{(S1)}
$$

The calculation expressions for the formation energies of all participating species are illustrated in **Table S3**, where E represents the generalized formation energy, U is the free

energy calculated by DFT, and R indicates the reference atomic species.

Table S3 List of all species involved in the reaction and corresponding formation energy calculation expressions.

Species	Calculation Expressions
C$_2$H$_4$ (gas)	$E_{C_2H_4} = U_{C_2H_4} - 2R_C - 4R_H$
O$_2$ (gas)	$E_{O_2} = U_{O_2} - 2R_O$
EO (gas)	$E_{EO} = U_{EO} - 2R_C - 4R_H - R_O$
AA (gas)	$E_{AA} = U_{AA} - 2R_C - 4R_H - R_O$
C$_2$H$_4$*	$E_{C_2H_4*} = U_{C_2H_4(surface)} - U_{(surface)} - 2R_C - 4R_H$
O*	$E_{O*} = U_{O(surface)} - U_{(surface)} - R_O$
O$_2$*	$E_{O_2*} = U_{O_2(surface)} - U_{(surface)} - 2R_O$
EO*	$E_{EO*} = U_{EO(surface)} - U_{(surface)} - 2R_C - 4R_H - R_O$
AA*	$E_{AA*} = U_{AA(surface)} - U_{(surface)} - 2R_C - 4R_H - R_O$
OME*	$E_{OME*} = U_{OME(surface)} - U_{(surface)} - 2R_C - 4R_H - R_O$
TS-OO	$E_{TSOO*} = U_{TSOO(surface)} - U_{(surface)} - 2R_O$
TS1	$E_{TS1*} = U_{TS1(surface)} - U_{(surface)} - 2R_C - 4R_H - R_O$
TS-EO	$E_{TSEO*} = U_{TSEO(surface)} - U_{(surface)} - 2R_C - 4R_H - R_O$
TS-AA	$E_{TSAA*} = U_{TSAA(surface)} - U_{(surface)} - 2R_C - 4R_H - R_O$

S5. Reaction kinetics including OME decomposition

Recently, Liu and co-workers have discovered that OME decomposition also belongs to one of the selective competition steps.[2] In order to gain a comprehensive understanding of the kinetics of ethylene epoxidation on silver surfaces, we have incorporated the OME decomposition process into the kinetic network, as detailed in **Table S4**. The OME decomposition process comprises two distinct steps: Step 8 involves the dehydrogenation of the intermediate OME, leading to the generation of the intermediate OxoE on the silver surface.

6

Step 9 subsequently generates adsorbed acetaldehyde (AA) from the intermediate OxoE and adsorbed hydrogen atoms. The OME decomposition step includes two transition states, namely the transition states of intermediate OxoE formation (TSOxoE) and the AA formation (TSAA2).

Table S4 The elementary steps utilized of this work and Liu and co-workers.[2] The red step represents the selective competition step. TSEO represents the transition state of EO formation. TSAA, TSAA1, and TSAA2 all represent the transition states of AA formation. TSOxoE represents the transition state of the intermediate OxoE formation.

	Two selective competition steps (This work)	Three selective competition steps (Liu and co-workers)[2]
1	$O_2(g) + 2* \leftrightarrow O_2**$	$O_2(g) + 2* \leftrightarrow O_2**$
2	$C_2H_4(g) + * \leftrightarrow C_2H_4*$	$C_2H_4(g) + * \leftrightarrow C_2H_4*$
3	$O_2** \leftrightarrow 2O*$	$O_2** \leftrightarrow 2O*$
4	$C_2H_4* + O* \leftrightarrow OME* + *$	$C_2H_4* + O* \leftrightarrow OME* + *$
5	$C_2H_4(g) + O* \leftrightarrow OME*$	$C_2H_4(g) + O* \leftrightarrow OME*$
6	$OME* \leftrightarrow EO*$ (TSEO)	$OME* \leftrightarrow EO*$ (TSEO)
7	$OME* \leftrightarrow AA*$ (TSAA)	$OME* \leftrightarrow AA1*$ (TSAA1)
8	-	$OME* + * \leftrightarrow OxoE* + H*$ (TSOxoE)
9	-	$OxoE* + H* \leftrightarrow AA2* + *$ (TSAA2)
10	$EO* \leftrightarrow EO(g) + *$	$EO* \leftrightarrow EO(g) + *$
11	$AA* \leftrightarrow AA(g) + *$	$AA1* \leftrightarrow AA1(g) + *$
12	-	$AA2* \leftrightarrow AA2(g) + *$

As presented in **Table S5**, the decomposition of OME exhibits a limited influence on both the reaction activity and selectivity. This can be attributed to the fact that the OME decomposition step involves two transition states, making the generation of AA2 relatively difficult compared to AA1. It is worth noting that the generation rate of AA2 is negligible. As a result, disregarding the OME decomposition step has a limited impact on the outcomes of our

kinetic studies.

Table S5 Table of TOF values and selectivity for product generation.

	TOF$_{EO}$	TOF$_{AA1}$	TOF$_{AA2}$	EO Selectivity
Two selective competition steps	3.411E-03	3.288E-05	-	99.05%
Three selective competition steps	3.411E-03	3.288E-05	1.307E-07	99.04%

S6. Additional energy profiles

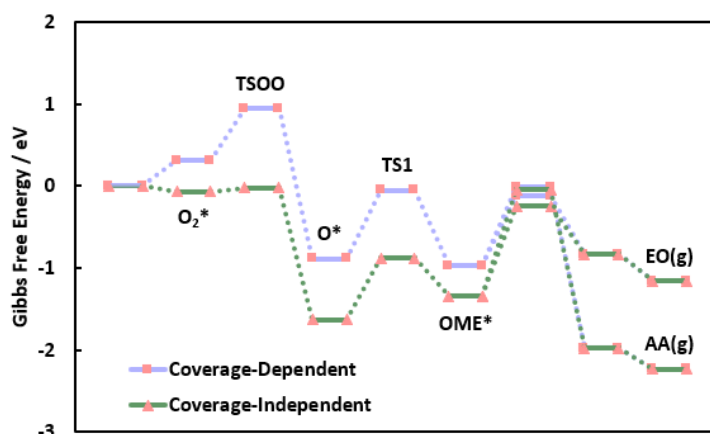**Figure S8** Free energy profiles of ethylene epoxidation on Cu(111) with E-R mechanism at 500 K, p_{O_2} = 20 kPa, and p_{Et} = 2.66 kPa.

S7. Degree of rate control (DRC) analysis of ethylene epoxidation

In order to gain a more precise understanding of the activity of ethylene epoxidation on the copper surface, we have applied coverage-dependent microkinetic modeling to analyze the reaction DRC on Cu(111) thoroughly. The purpose of DRC analysis is to provide explicit insight into the degree of influence of each elementary step on the overall reaction activity. If the DRC of an elementary step is non-zero, it has an impact on the overall reaction rate. A positive value of DRC suggests that the step is rate-controlling, while a negative value of DRC indicates that the step is rate-inhibiting. The sum of the DRC values that affect the same

8

elementary step is unity, and the elementary step with the highest DRC is known as the rate-determining step. In this work, we have focused on two of the most critical elementary steps, namely the ethylene epoxide formation (step 6: OME* → EO*) and the acetaldehyde formation (step 7: OME* → AA*). The DRC results for the selective competition step (step 6 and step 7) are presented in **Figure S9**.

Firstly, **Figure S9** (a) presents a comprehensive analysis with coverage-dependent microkinetic modelings of the ethylene epoxide formation step. Based on the analysis, it was found that, except for the self-interaction of ethylene epoxide formation (step 6: OME* → EO*), oxygen dissociation (step 3: O_2** → 2O*) has the most significant impact on the rate of ethylene epoxide formation. The DRC of oxygen dissociation was observed to be positive, indicating that the rate of EO generation will increase with the decline in the oxygen dissociation energy barrier. On the other hand, the DRC of the acetaldehyde formation step (step 7: OME* → AA*) was found to be the only negative value, which has an inhibitory effect on the rate of ethylene epoxide generation. This observation is well understood because the ethylene epoxide formation step and the acetaldehyde formation step are selective competition steps.

The formation of acetaldehyde is affected by several variances, as depicted in **Figure S9** (b). Among these variances, the oxygen dissociation barrier has a similar effect on the DRC of acetaldehyde formation as on the ethylene epoxide formation. The opposite sign indicates that selective competition steps have inhibitory cross-interactions. The DRC performance of the selective competition step that affects the rate of AA production is more severe than that of EO production. The selectivity of ~90% EO in the product is the primary reason for the difference in the absolute value of the DRC in the selective competition step, which robustly suppresses the selectivity and activity of AA. Based on this, the AA reaction activity is more sensitive to the influence in the selective competition step.
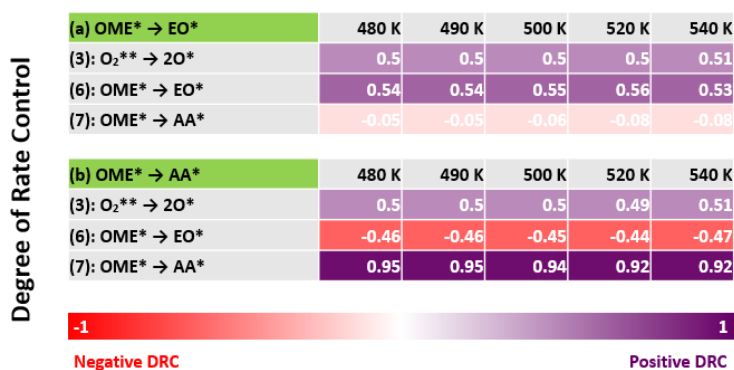
Degree of Rate Control

(a) OME* → EO*	480 K	490 K	500 K	520 K	540 K
(3): O_2** → 2O*	0.5	0.5	0.5	0.5	0.51
(6): OME* → EO*	0.54	0.54	0.55	0.56	0.53
(7): OME* → AA*	-0.05	-0.05	-0.06	-0.08	-0.08

(b) OME* → AA*	480 K	490 K	500 K	520 K	540 K
(3): O_2** → 2O*	0.5	0.5	0.5	0.49	0.51
(6): OME* → EO*	-0.46	-0.46	-0.45	-0.44	-0.47
(7): OME* → AA*	0.95	0.95	0.94	0.92	0.92

-1		1
Negative DRC		Positive DRC

Figure S9 DRC analysis of ethylene epoxidation on Cu(111) at p_{Et} = 588 kPa and p_{O_2} = 47 kPa. (a) represents the pathway of ethylene epoxide formation. (b) exhibits the channel of acetaldehyde formation. Hints: Only surface reactions are included, while the fast-equilibration step does not affect reaction DRC.

References

1   A. J. Medford, C. Shi, M. J. Hoffmann, A. C. Lausche, S. R. Fitzgibbon, T. Bligaard and J. K. Nørskov, *Catal. Letters*, 2015, **145**, 794–807.

2   D. Chen, P. L. Kang and Z. P. Liu, *ACS Catal.*, 2021, **11**, 8317–8326.